Bull. Mater. Sci. (2019) 42:120
https://doi.org/10.1007/s12034-019-1783-7

Superoxide dismutase mimic activity of spinel ferrite MFe_2O_4 (M = Mn, Co and Cu) nanoparticles

VIBHA VERMA[1,*], MANPREET KAUR[1] and SUCHETA SHARMA[2]
[1]Department of Chemistry, Punjab Agricultural University, Ludhiana 141 004, India
[2]Department of Biochemistry, Punjab Agricultural University, Ludhiana 141 004, India
*Author for correspondence (rana.vibz22@gmail.com)

MS received 10 May 2018; accepted 27 November 2018; published online 24 April 2019

Abstract. In the present study, superoxide dismutase (SOD) mimic activity of ferrite nanoparticles (NPs), having a formula MFe_2O_4 (M = Mn, Co and Cu) was investigated. Spinel ferrite NPs were synthesized by employing sol–gel methodology and characterized using scanning electron microscopy, X-ray diffraction, BET analysis and Fourier transform infrared spectroscopy techniques. BET analysis revealed that the surface area of ferrite NPs ranged from 0.43−23.49 $m^2\ g^{-1}$. Enzyme mimic activity was compared using SOD as a model enzyme. $CuFe_2O_4$ NPs exhibited a maximum activity followed by $CoFe_2O_4$ and $MnFe_2O_4$ NPs. The results were correlated with a facile interconversion of the oxidation state leading to a stable electronic configuration in $CuFe_2O_4$ NPs. Optimum pH and contact time was 1 and 3 min respectively. Kinetic studies were performed under optimum conditions and data were analysed using the Michaelis Menten equation. The values of V_{max} (0.77 s^{-1}) and K_m (4.20 mM) proved $CuFe_2O_4$ NPs as potential SOD mimic for a wide range of applications.

Keywords. Ferrite nanoparticles; enzyme mimics; superoxide dismutase mimic.

1. Introduction

Enzyme mimics are an upcoming area of research due to their high stability, cost effectiveness, tunable catalytic properties and easy handling and storage in comparison with natural enzymes. They have gathered attention due to their immense commercial potential over their natural counterparts. Although natural enzymes possess efficient catalytic activity, high selectivity and substrate specificity, but their efficiency and stability is severely affected by environmental conditions, denaturation and digestion, thus limiting their commercial applications [1,2]. Moreover, they are difficult to prepare, purify and store, thus making artificial enzymes preferable over the natural ones. Nowadays they have been applied in the area of environmental protection, chemical/biological sensors, cancer treatment, anti-fouling systems, in pharmaceutical and fuel industries etc. [3–5]. The basic approaches to design the artificial enzymes are either to reproduce enzyme active sites or mimic the chemical reaction i.e., chemical transformation of reactants to products without copying the structure of enzyme active sites.

A superoxide (O_2^-) anion produced from one electron reduction of molecular oxygen plays a major role in oxidative stress. It also affects the production of other reactive species like peroxynitrite (ONOO–) and its degradation products (OH, CO_3^- and NO_2), H_2O_2, lipid alkoxyl (RO) and peroxyl (RO_2) radicals. Excess of these reactive species results in redox imbalance leading to excessive immune responses, inflammation and various diseases such as complications of diabetes, stroke, reperfusion injury and rheumatoid arthritis [6]. H_2O_2 resulting from one-electron reduction of superoxide is a dominant signalling molecule. Thus, endogenous antioxidants are essential to maintain reactive species at nanomolar levels. The superoxide dismutase (SOD) family comprises MnSOD and FeSOD located in the mitochondrial matrix and chloroplasts respectively and Cu–Zn SOD is located in the mitochondrial intermembrane space, extracellular space and cytosol. This metalloenzyme eliminates the superoxide anion by catalysing its dismutation i.e. disproportionation to molecular oxygen and hydrogen peroxide, and thus acts in primary internal anti-oxidant defence of the body [7]. However, its use as an anti-oxidant is not only limited to biological reactions but also to various fields like food processing, medical applications, cosmetics and plant industries [8–10]. This encouraged the development of synthetic SOD mimic as an anti-oxidant. To date, a wide range of synthetic molecules like manganese and porphyrin based complexes have been explored as SOD mimics [11].

In the last few decades, the potential use of nanoparticles (NPs) has been studied as enzyme mimics due to their high surface to volume ratio [12–14]. To date a wide range of NPs have been exploited for their enzyme mimic activity [15–17]. Among them, magnetic NPs have proved a powerful tool as enzyme mimics for applications in the field of environmental chemistry, medicines and biotechnology [17–20]. SOD mimic activity of manganese complexes has been widely studied due to their high stability and low toxicity [21]. However, to the best of our knowledge no work has

been performed on SOD mimic activity of ferrite NPs. Thus, in the present work, SOD mimic activity of spinel ferrite MFe_2O_4 NPs (M = Mn, Co and Cu) was studied. The effect of changing a metal ion in a spinel lattice on SOD mimic activity was observed and detailed investigation on the effect of reaction conditions on activity was recorded. Kinetic studies were performed and kinetic parameters were determined using the Michaelis Menten equation.

2. Experimental

2.1 *Materials*

Chemicals used *viz*., $Mn(NO_3)_2{\cdot}6H_2O$, $Co(NO_3)_2{\cdot}6H_2O$, $Cu(NO_3)_2{\cdot}6H_2O$, $Fe(NO_3)_3{\cdot}9H_2O$, citric acid, NH_4OH, pyrogallol and ethylene diaminetetraacetic acid (EDTA) were of AR grade. The pH of reaction solution was adjusted using 0.1 N HCl and 0.1 N NaOH. Double distilled water was used to prepare the solutions.

2.2 *Instrumentation*

X-ray diffraction (XRD) and Fourier transformed infrared spectroscopy (FT-IR) analyses were performed with a Panalytical X'pert Pro using CuK_α radiation ($\lambda = 1.5404$ Å) and a Thermo Nicolet 6700 FT-IR Spectrometer. Scanning electron microscopy of ferrite nanoparticles (NPs) was performed by employing Hitachi S-3400 N and EDX on a Thermo Noran System SIX respectively. BET isotherms were analysed using a Quantachrome Nova-1000 surface analyser under liquid nitrogen atmosphere. The measurements of enzyme mimic activity were performed using a UV-1800 Shimadzu Double-beam Spectrophotometer.

2.3 *Synthesis of ferrite NPs*

Ferrite NPs were synthesized using a sol–gel method [22]. Stoichiometric amounts of metal nitrates were dissolved in double distilled water, followed by the addition of an equimolar amount of citric acid as a chelating agent to the reaction mixture. Ammonia solution was added slowly to adjust the pH of the reaction mixture to 8.0 and the mixture was continuously stirred at 60−70°C. After 3 h, the sol was transformed into black gel which was dried at 100°C in an oven for 8 h. After drying, its volume expanded four times. The dried gel was calcined for 3 h at 300°C to obtain the final thermolysis product.

2.4 *SOD like activity of ferrite NPs*

Ferrite NPs were tested for SOD mimic activity using the Marklund and Marklund method at 25°C [23]. SOD/SOD mimics catalyse the dismutation of the superoxide anion (formed during pyrogallol auto-oxidation) into hydrogen peroxide. The resulting oxidized product showed an absorbance

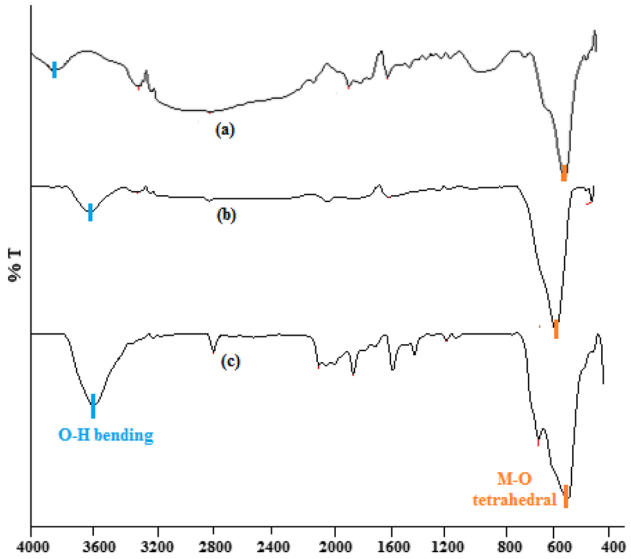

Figure 1. FT-IR spectra of (**a**) $MnFe_2O_4$, (**b**) $CoFe_2O_4$ and (**c**) $CuFe_2O_4$ NPs.

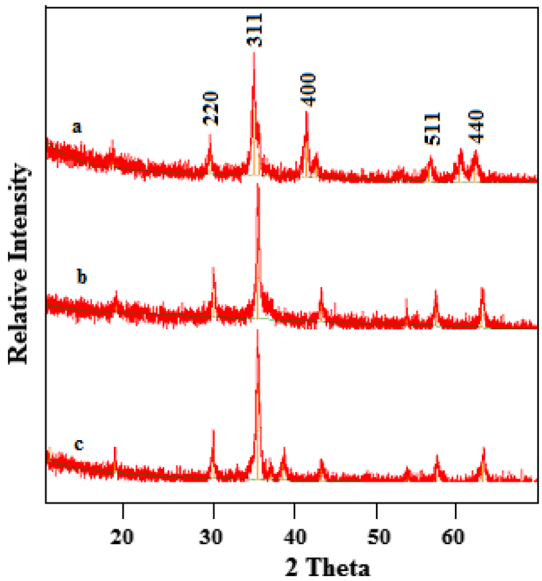

Figure 2. XRD pattern of (**a**) $MnFe_2O_4$, (**b**) $CoFe_2O_4$ and (**c**) $CuFe_2O_4$ NPs.

maximum (λ_{max}) at 420 nm. Lesser the value of absorbance, more the dismutation of the superoxide anion, and greater is the SOD mimic activity. The effect of the presence of MFe_2O_4 NPs on the absorbance of the reaction mixture was observed. The activity of MFe_2O_4 NPs was compared on the basis of the absorbance value when experiments were carried out at different pH values, temperatures, catalysts and substrate concentrations to evaluate the effect of various parameters.

Table 1. XRD parameters of ferrite NPs.

Material code	Composition	Lattice constant (Å)	X-ray density (g cc^{-1})	Physical density (g cc^{-1})	% Porosity	Average particle diameter (nm)
a	$MnFe_2O_4$	8.424	5.123	3.81	25.58	17.75
b	$CoFe_2O_4$	8.343	5.365	2.96	44.82	18.98
c	$CuFe_2O_4$	8.321	5.514	3.44	37.56	19.43

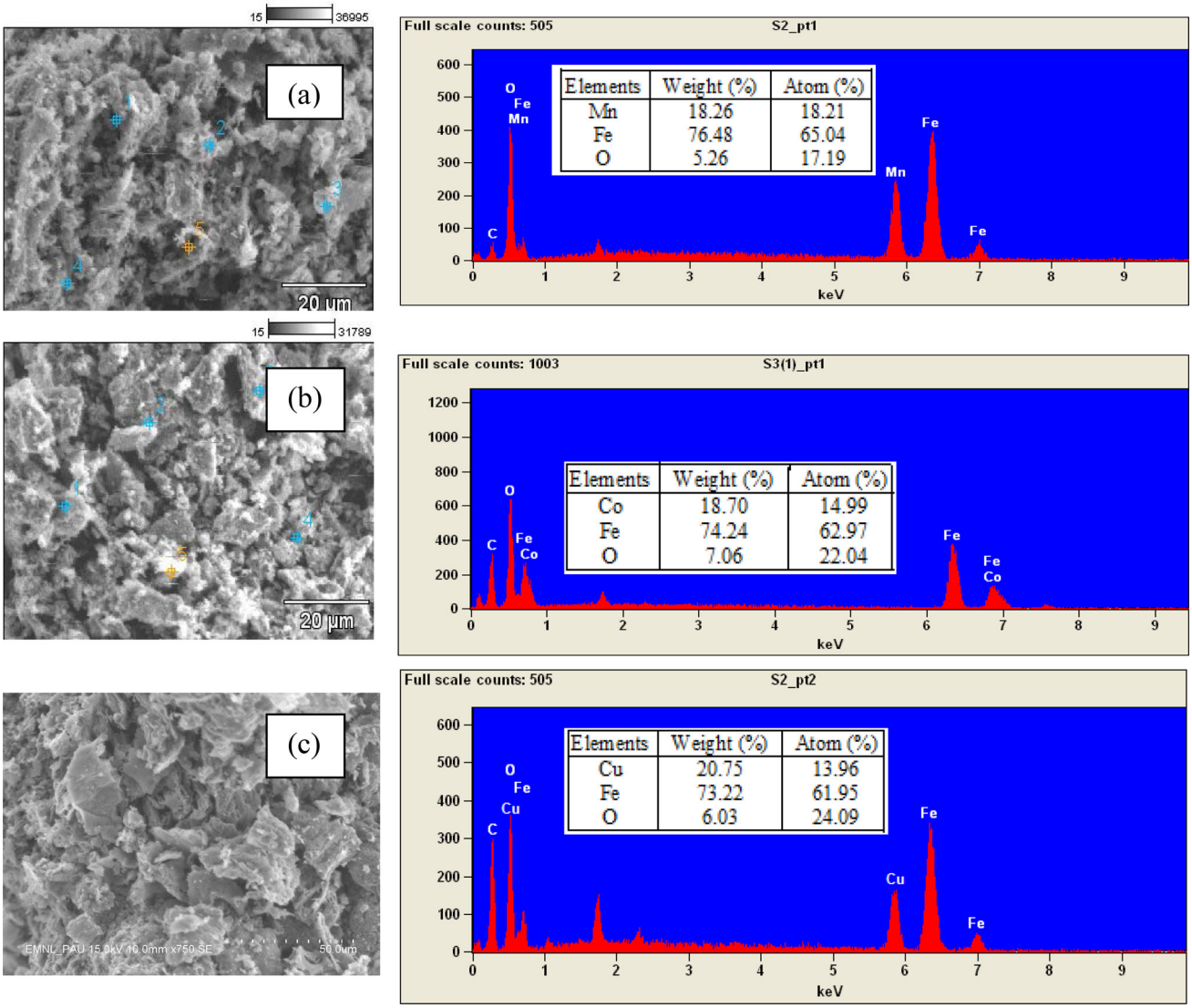

Figure 3. SEM–EDX micrographs of (**a**) $MnFe_2O_4$, (**b**) $CoFe_2O_4$ and (**c**) $CuFe_2O_4$ NPs.

The SOD mimic activity was assayed in a spectrophotometric cuvette having a reaction volume of 3 ml containing 2 ml (6 mM) pyrogallol and 1 ml (6 mM) EDTA. Both the contents were mixed and pH of the reaction mixture was adjusted to optimize the value of 8.2 using 0.1 N NaOH solution. The reaction started on adding 1 mg ferrite NP into the solution. The mixture was subjected to atmospheric oxygen for 3 min and the colorimetric analysis was performed spectrophotometrically. A reaction mixture without ferrite NPs was used as blank. The activity of enzyme mimic is expressed in activity unit (A.U.) where 1 A.U. is equivalent to 50% inhibition of pyrogallol oxidation as compared to blank. For steady-state kinetic parameters of ferrite NPs, under optimum conditions i.e. pH = 1 with a dose of 2 mg of NPs for 3 min, the absorbance of the reaction mixture was noted with varying concentrations of the

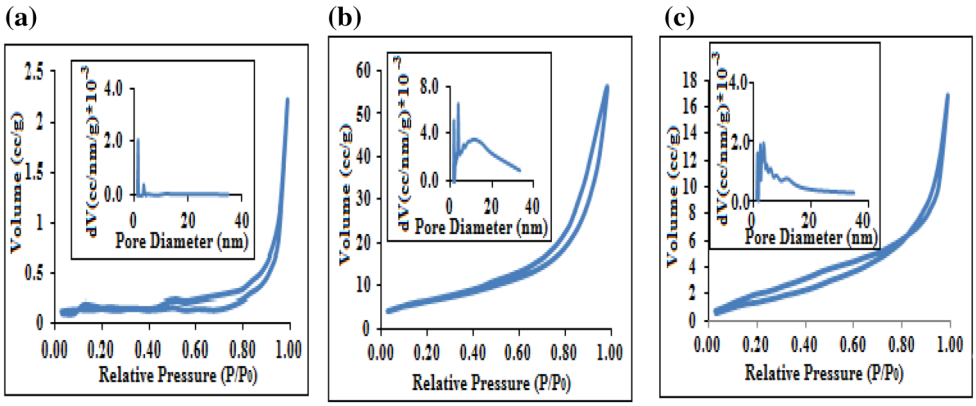

Figure 4. BET isotherms of ferrite NPs (**a**) $MnFe_2O_4$, (**b**) $CoFe_2O_4$ and (**c**) $CuFe_2O_4$ NPs.

substrate. The reactions were monitored using time scan mode at 420 nm. The absorbance data were fitted in the Michaelis–Menten equation as described below

$$v = \frac{v_{max}[S]}{K_m + [S]} \quad (1)$$

where v is the rate of the reaction, v_{max} is the maximum rate of the reaction and $[S]$ is the substrate concentration. K_m is the Michaelis constant which indicates the affinity of the enzyme towards the substrate and is equivalent to the substrate concentration at which the rate of conversion is half of v_{max}. Lower the value of K_m, higher the enzyme mimic activity. The values of K_m and v_{max} were calculated by plotting the Lineweaver–Burk plot between $1/[S]$ and $1/v$. The intercept on x- and y-axes gave values of K_m and v_{max}, respectively.

3. Results

3.1 *Characterization*

In FT-IR spectra of ferrite NPs (figure 1) the peaks appeared in the range of 548.36−576.18 cm^{-1} and 3434.42−3774.69 cm^{-1} that corresponded to the vibration of the metal oxygen (M–O) bond in the tetrahedral sites and O–H stretching of adsorbed water molecules respectively [24]. The XRD patterns of ferrite NPs (figure 2) showed well defined peaks in the crystallographic planes of (220), (311), (400), (511) and (440) which were confirmed by matching with ASTM Data Card no. 10-319, 3-0865 and 25-283. XRD parameters and the particle size calculated from Scherrer's formula are reported in table 1.

SEM–EDX of NPs using a point and shoot method was recorded at 15 kV at different points and EDX spectra with elemental composition are shown in figure 3. The spectra showed the relative effective atomic concentrations of different constituents in different ferrite NPs (peak of C due to carbon stub). The surface morphology was studied using SEM micrographs and was found to be porous.

Table 2. BET surface area of ferrite NPs.

Material code	Pore volume (cc g^{-1})	Pore diameter (nm)	Surface area (m^2 g^{-1})
a	0.002	1.561	0.433
b	0.081	3.630	23.498
c	0.021	3.642	8.897

Nitrogen adsorption and desorption measurements of the samples were used to evaluate porosity and the specific surface area (figure 4). The BET surface area of $MnFe_2O_4$, $CoFe_2O_4$ and $CuFe_2O_4$ NPs was found to be 0.433, 23.498 and 8.897 m^2 g^{-1} respectively and the total pore volume was 0.002, 0.081 and 0.021 cc g^{-1} respectively (table 2). The surface area played an important role in the observed trend of activity. More the surface area of ferrite NPs, more the sites available for substrate attachment and hence higher was the activity.

3.2 *Evaluation of SOD mimic activity of MFe_2O_4*

3.2a *Effect of pH*: For evaluating the effect of pH on SOD mimic activity, the pH of the reaction mixture was varied from 3.0–10.0 using 0.1 N HCl and 0.1 N NaOH and absorbance was noted after 10 min. It was observed that the activity of ferrite NPs first decreased on increasing the pH up to 8.0 (figure 5(a)) as indicated by higher absorbance values of the solution and subsequently increase which was affirmed by lowering in absorbance value at pH > 8. The results might be due to interaction of H^+ ions with O_2^- which inhibits its binding with metal ion containing SOD/SOD mimic.

3.2b *Comparison of SOD mimic activity of ferrite NPs*: The addition of $CuFe_2O_4$ NPs resulted in a maximum lowering in absorbance of the reaction mixture followed by $CoFe_2O_4$ and $MnFe_2O_4$ NPs. The results were correlated with the inter-conversion of the oxidation state during superoxide dismutation. The highest activity of $CuFe_2O_4$ NPs

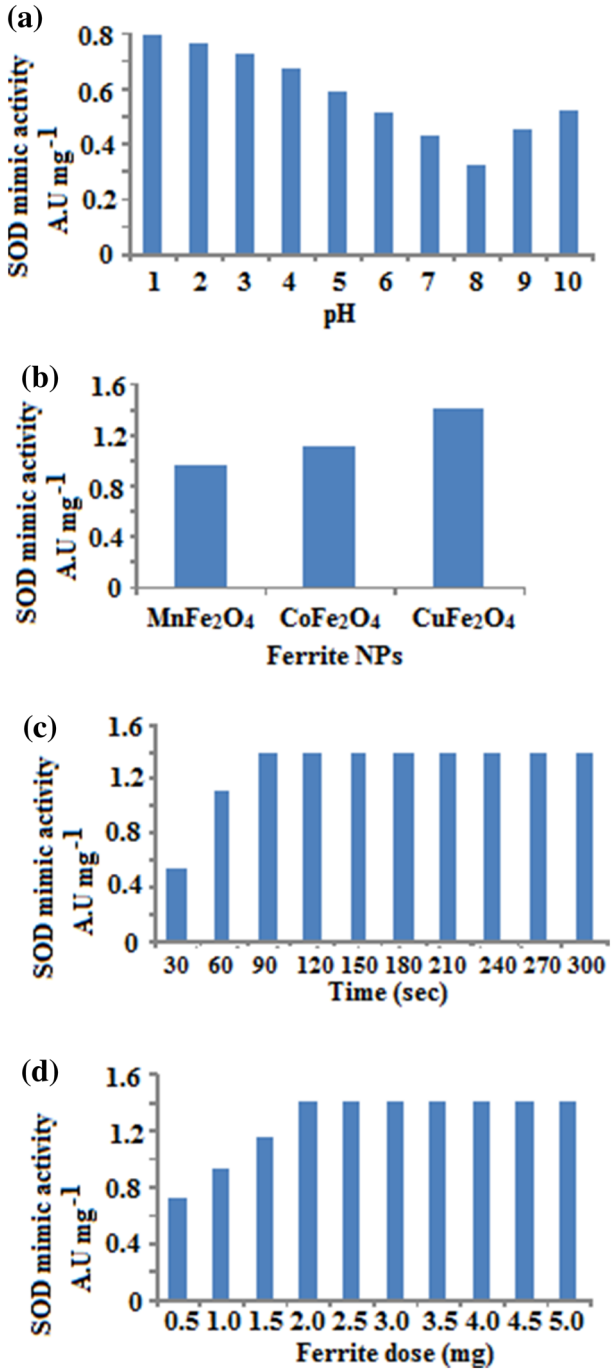

Figure 5. (**a**) Effect of pH on SOD mimic activity of $CuFe_2O_4$ NPs, (**b**) comparison of SOD mimic activity of ferrite NPs, (**c**) effect of contact time on SOD mimic activity of $CuFe_2O_4$ NPs and (**d**) effect of $CuFe_2O_4$ NP dose on SOD mimic activity.

can be attributed to the facile conversion of Cu^{2+} to Cu^{+} due to the electron transfer from a substrate containing superoxide radical to $CuFe_2O_4$ NPs that lead to more stable $3d^{10}$ configurations from $3d^9$ configurations. Whereas, in the case of $CoFe_2O_4$ and $MnFe_2O_4$ NPs the change in the oxidation state from +2 to +1 did not lead to a favourable electronic configuration. A similar mechanism is reported in

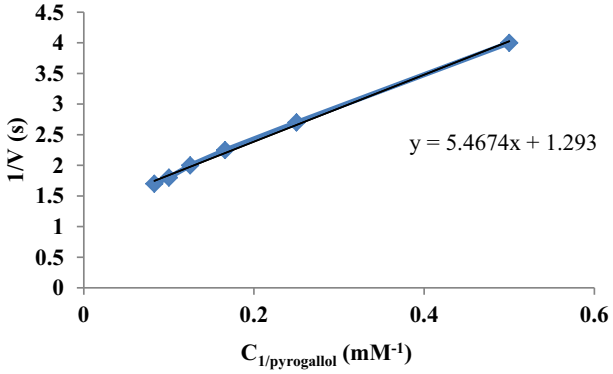

Figure 6. Steady-state kinetic assay of SOD mimic activity of $CuFe_2O_4$ NPs.

the case of the Cu–Zn SOD enzyme during dismutation of the O_2^- anion [25]. The higher activity of $CoFe_2O_4$ as compared to $MnFe_2O_4$ NPs might be explained on the basis of the higher surface area of the former which resulted in more available reactive sites for the attachment of substrates and thus scavenging the superoxide radicals at a faster rate (figure 5(b)).

3.2c *Effect of contact time and catalyst dose of ferrite NPs*: To observe the effect of contact time, SOD mimic activity was evaluated for 10 min at an interval of 30 s. The results showed that the maximum activity was achieved within 3 min, afterwards, no significant change in activity was observed. Thus, for subsequent experiments the value of absorbance was noted after 3 min (figure 5(c)).

In the reaction mixture, ferrite NPs (0.5–5 mg) were added. The activity first increased on addition of ferrite NPs up to 2 mg followed by a non-significant change in absorbance up to 5 mg (figure 5(d)). The increase in activity on increasing dose of NPs was due to availability of more active sites, but at an optimum dose of 2 mg the substrate was saturated on the active sites of NPs and further increase in the dose of NPs did not result in any increase in activity. Thus, 2 mg of NPs for 3 ml reaction solution (0.66 mg ml^{-1}) was the optimum enzyme mimic dose.

3.2d *Steady-state kinetics*: To investigate the catalytic mechanism of $CuFe_2O_4$ NPs, apparent steady-state kinetic parameters for the SOD mimic reaction were measured using pyrogallol as the substrate. The parameters were obtained by varying the substrate concentrations. The slope and intercept of the graph gave the value of the maximum velocity (υ_{max}) and Michaelis Menten constant (K_m) (figure 6). The υ_{max} and K_m obtained were 0.77 s^{-1} and 4.20 mM respectively which were comparable to the reported value for SOD enzyme values in the literature [26]. The optimum pH for naturally available SOD is 9, whereas ferrite nanoparticles showed a maximum SOD like activity at pH 1. Thus the direct comparison was not undertaken as SOD and ferrite NPs did not show a maximum activity under identical conditions of pH due to

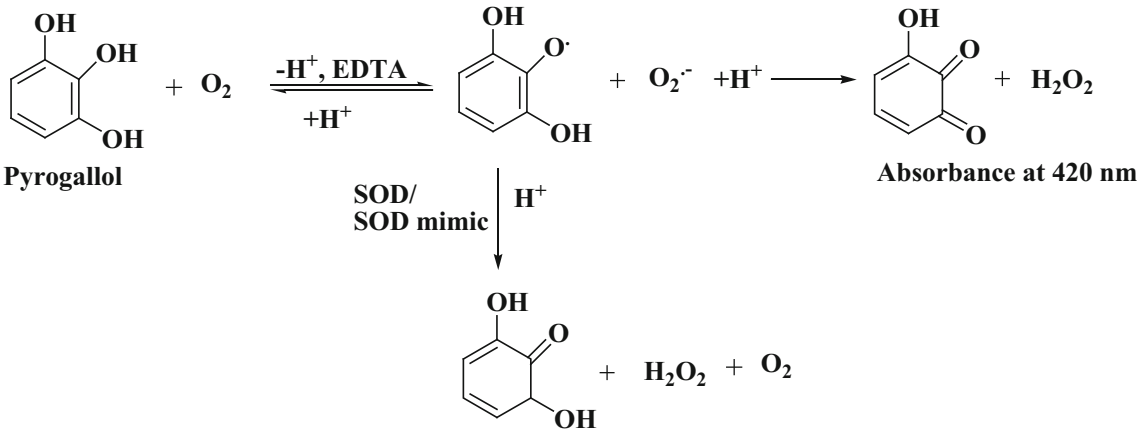

Scheme 1. Proposed mechanism of SOD/SOD mimic activity.

difference in their structural features. Therefore activity was compared with the reported values for SOD in the literature. The proposed catalytic mechanism is shown in scheme 1. The superoxide anion first binds to Cu^{2+} of ferrite NPs and reduces Cu^{2+} to Cu^{+}. Further protonation resulted in the loss of dioxygen and the conversion of Cu^{+} back to Cu^{2+}.

4. Conclusions

In the present study, the effect of a metal ion in spinel ferrite NPs on SOD mimic activity was observed. A facile sol–gel method was used to synthesize MFe_2O_4 NPs (M = Mn, Co and Cu). Although, all the synthesized ferrite NPs showed SOD mimic activity, the ferrite NPs containing Cu^{2+} as a divalent ion showed a maximum SOD mimic activity followed by $CoFe_2O_4$ and $MnFe_2O_4$ NPs. The observed trend was attributed to the facile conversion of Cu^{2+} to Cu^{+} that led to a more stable configuration. The higher activity of $CoFe_2O_4$ as compared to $MnFe_2O_4$ NPs was explained on the basis of the higher surface area of the former that provided more reactive sites. Kinetic analysis of $CuFe_2O_4$ NPs confirmed the potential of $CuFe_2O_4$ as a SOD mimic.

Acknowledgements

The authors are thankful to EMN lab Punjab Agricultural University, Ludhiana for SEM–EDX recordings.

References

[1] Kuah E, Toh S, Yee J, Ma Q and Gao Z 2016 *Chemistry* **22** 8404
[2] Breslow R 1982 *Science* **218** 532
[3] Wiseman A 1993 *J. Chem. Technol. Biotechnol.* **56** 3
[4] Yang B, Li J, Deng H and Zhang L 2016 *Crit. Rev. Anal. Chem.* **46** 469
[5] Cormode D P, Gao L and Koo H 2018 *Trends. Biotechnol.* **36** 15
[6] Christianson D W 1997 *Prog. Biophys. Mol. Biol.* **67** 217
[7] Vecchio G and Lanza V 2009 *J. Chem. Edu.* **86** 1419
[8] Donnelly J K, McLellan K M, Walker J L and Robinson D S 1989 *Food Chem.* **33** 243
[9] Soulere L, Delplace P, Davioud-Charvet E, Py S and Sergheraert C 2003 *Bioorg. Med. Chem.* **11** 4941
[10] Gopal R K and Sanniyasi E K 2017 *J. Prob. Health* **5** 179
[11] Batinić-Haberle I, Rebouc J S and Spasojević I 2010 *Antioxid. Redox Signal.* **13** 877
[12] Hu X, Liu J, Hou S, Wen T, Liu W *et al* 2011 *Sci. China. Phys. Mech.* **54** 1749
[13] Gao L, Fan K and Yan X 2017 *Theranostics* **7** 3207
[14] Hu A, Deng H, Zheng X, Wu Y, Lin X *et al* 2017 *Biosens. Bioelectron.* **97** 21
[15] Wang C, Chen W and Chang H 2012 *Anal. Chem.* **84** 9706
[16] Maria J R and Elizabeth A H 2010 *Anal. Chem.* **82** 9043
[17] Yang W, Hao J, Zhang Z and Tang J 2014 *RSC Adv.* **4** 35500
[18] Luo L, Zhang Y, Li F and Wang T 2013 *Anal. Chim. Acta* **788C** 46
[19] Chen Z, Yin J J, Zhou Y T, Zhang Y, Song L *et al* 2012 *ACS Nano* **6** 4001
[20] Wang H, Li S, Si Y, Sun Z, Lia S and Lin Y 2014 *J. Mater. Chem. B* **2** 4442
[21] Miriyala S, Spasojevic I, Tovmasyan A, Salvemini D, Vujaskovic Z *et al* 2012 *Biochim. Biophys. Acta* **1822** 794
[22] Kaur N and Kaur M 2014 *Process. Appl. Ceram.* **8** 137
[23] Marklund S and Marklund G 1974 *Eur. J. Biochem.* **47** 469
[24] Kaur M, Jain P and Singh M 2015 *Mater. Chem. Phys.* **162** 332
[25] Pelmenschikov V and Siegbahn P E M 2005 *Inorg. Chem.* **44** 3311
[26] Asthir B, Koundal A and Bains N S 2011 *Indian. J. Biochem. Bio.* **48** 341